Comparison of three filters in the solution of the Navier-Stokes equation in registration

C. Gramkow[1,3] and M. Bro-Nielsen[1,2,3]
[1]IMM - Department of Mathematical Modelling,
Technical University of Denmark, Bldg. 321
2800 Lyngby, Denmark,
[2]HT Medical, Inc.
6001 Montrose Road, Suite 902,
Rockville, MD 20852, USA.
[3]3D-Lab, Panum Institute,
University of Copenhagen, 2200 N, Denmark,
email: cgr@imm.dtu.dk, bro@ht.com

Abstract

The registration of images is an often encountered problem in e.g. medical imaging, satelite imaging, or stereo vision. In most applications a rigid deformation model does not suffice and complex deformations must be estimated. In medical registration *Bajcsy et al.* [1] have proposed the use of elastic models to describe the registration. *Christensen et al.* [3, 4, 5, 6, 8] proposed the use of fluid models that lack some of the constraints of the elastic model. They solve the viscous partial differential equation (PDE), which is the core problem of the fluid model, using the computationally expensive Succesive Over-Relaxation (SOR) algorithm. *Thirion* [9] calculated a flow velocity by regularizing the derived driving forces by a gaussian convolution filter. In this paper we propose an elastic filter to be used in convolution to approximate the solution of Navier-Stokes equation, and we compare the performance of the derived filter with two other filters, a separable approximation to the elastic filter and the well-known gaussian proposed by *Thirion*. The convolution approach is several times faster than the SOR algorithm.

keywords: registration, Navier-Stokes equation, convolution, elasticity filter.

1 Introduction

To relate information in two images, aquired from different modalities and in different reference frames, requires a mathematical mapping between the two images coordinate systems. The estimation of such a map is called a registration of the images. The registration of images is an often encountered problem in e.g. medical imaging, satelite imaging, or stereo vision. In the medical field the objective could be to relate information in different images, to observe changes over periods of time, or statistically to describe anatomical differences [8]. These tasks require that the involved images are registered with each other. The registration can be modelled as a deformation or warping of one image into a best fit with the other image. Due to the anatomical variability in inter-patient studies a non-linear deformation model must be employed. In recent years *Bajcsy and Kovačič* [1] and *Christensen et al.* [3, 4, 5, 6, 8] have proposed the use of elastic and fluid deformation models, i.e. the mathematical map between the images is constrained by the laws of elastic or fluid materials. The latter has the advantage that it allows for large curved deformations, which do not appear in elastic models. Unfortunately, the fluid model requires the repeated solution of Navier-Stokes equation, which governs the instantaneous velocity of the deformation flow and the applied force. In *Christensen* [3] this equation is solved using the Succesive Over-Relaxation (SOR) algorithm, which is an iterative scheme where checker-board updates are performed. This algorithm is computationally expensive.

Bro-Nielsen and Gramkow [2, 7] proposed the use of convolution to approximate the solution of Navier-Stokes equation, and presented Christensen's fluid registration algorithm in a multi-resolution framework. *Thirion* [9] presents an iterative algorithm where the derived image forces are regularized by gaussian smoothing. The smoothed forces are then used directly as the instantaneous flow estimate in an Euler integration. Thus, the latter approach by *Thirion* uses a gaussian regularizer whereas the method developed by *Christensen* uses an elastic model regularizer.

In this paper we compare the performance of our derived elastic convolution filter with two other filters. The first is a separable approximation to the derived filter and the other is the well-known gaussian proposed by *Thirion* [9]. The paper will show that the choice of regularization method has a large influence on the registration result. This should not be underestimated when choosing a regularizer.

In this paper the registration quality is validated as the ability of the method to estimate a smooth regular homeomorphic map between two synthetic images. No quantitative results are given. The reader is referred to *Christensen* [3], *Thirion* [9], and *Gramkow and Bro-Nielsen* [7, 2] for anatomical examples of the performance of the methods.

2 The Fluid Model

The complete fluid model is out of the scope of this paper, but can be found in *Christensen* [3]. In *Bro-Nielsen and Gramkow* [2, 7] the model is described in a multi-resolution framework. The registration is obtained in an iterative scheme, where the deforming image locally deforms in the direction that gives the best fit with the other image. Thus, the force driving the deformation is derived from local image characteristics. The relation between the driving force $\boldsymbol{b}(\boldsymbol{x}, \boldsymbol{u}(\boldsymbol{x}, t))$ and the instantaneous velocity $\boldsymbol{v}(\boldsymbol{x}, t)$ of the deformation field $\boldsymbol{u}(\boldsymbol{x}, t)$ at time t is governed by Navier-Stokes equation

$$\alpha \nabla^2 \boldsymbol{v}(\boldsymbol{x}, t) + (\alpha + \beta) \nabla (\nabla^T \cdot \boldsymbol{v}(\boldsymbol{x}, t)) + \boldsymbol{b}(\boldsymbol{x}, \boldsymbol{u}(\boldsymbol{x}, t)) = \boldsymbol{0}, \tag{1}$$

where $\boldsymbol{x} = (x_1, x_2)$ is the image coordinate. The laplace operator in the first term causes the velocity field to be smooth, and the second term limits the gradient of the divergence of the field. Thus, the viscosity coefficients α and β represent the smoothness and the mass injection or compressibility of the material, respectively. Note, that the two first terms represent the internal forces which are in equilibrium with the external image forces in the last term. Basicly, the equation favors velocity fields with small second order variations. The deformation increment $\Delta \boldsymbol{u}(\boldsymbol{x}, t)$ is determined through simple Euler integration of the velocity

$$\boldsymbol{v}(\boldsymbol{x}, t) = \frac{\partial \boldsymbol{u}(\boldsymbol{x}, t)}{\partial t} + \nabla \boldsymbol{u}(\boldsymbol{x}, t) \boldsymbol{v}(\boldsymbol{x}, t) \tag{2}$$

The chain rule of differentiation must be applied, when the deformation is defined in the Eulerian reference frame. The driving force is derived from a cost measure, based on a Gaussian sensor model, and is calculated as

$$\boldsymbol{b}(\boldsymbol{x}, \boldsymbol{u}(\boldsymbol{x}, t)) = (T(\boldsymbol{x} - \boldsymbol{u}(\boldsymbol{x})) - S(\boldsymbol{x}) \nabla T|_{\boldsymbol{x} - \boldsymbol{u}(\boldsymbol{x})}, \tag{3}$$

where $T(\boldsymbol{x} - \boldsymbol{u}(\boldsymbol{x}))$ denotes the pixel-value of the deforming (template) image and $S(\boldsymbol{x})$ denotes the value of the study image. The above equations are applied iteratively until a stop criterion is satisfied. This may either be defined through the cost function or by a limit on the extent of deformation.

3 The Convolution Filter Solution

In this section we explain how a solution to equation 1 can be obtained be linear convolution. We design a linear filter that is used to solve the viscous PDE (1) by taking advantage of the linearity of the operator $\mathcal{L}$, that is imposed on the velocity field in equation 1

$$\mathcal{L} \boldsymbol{v} = \alpha \nabla^2 \boldsymbol{v} + (\alpha + \beta) \nabla (\nabla^T \cdot \boldsymbol{v}) \tag{4}$$

Using this operator equation 1 takes the form

$$\mathcal{L} \boldsymbol{v}(\boldsymbol{x}, t) + \boldsymbol{b}(\boldsymbol{x}, \boldsymbol{u}(\boldsymbol{x}, t)) = 0 \tag{5}$$

This operator is of the same form as the linear operator of elasticity in Hooke's law.

We derive a linear filter as an approximation to the impulse response of an applied force, and use this filter to determine the instantaneous velocity field around each image force. Due to the linearity of the operator the total velocity field is determined, through convolution, as the superposition of the responses for all forces. In fact, the filter is a discrete approximation to the Green's function for the operator $\mathcal{L}$.

We base the filter derivation on eigenfunction analysis. *Christensen* [3] has derived the eigenfunctions of (4) in his work on elastic registration. The eigenfunctions $\boldsymbol{\phi}_{ijr}(\boldsymbol{x})$ satisfy the equations

$$\mathcal{L}\phi_{ijr} = \kappa\phi_{ijr}, \qquad r = 1,2 \quad i,j \geq 0 \tag{6}$$

Under the Dirichlet boundary conditions

$$\begin{aligned} \phi_1(0,x_2) &= \phi_1(1,x_2) = 0 & (7)\\ \phi_2(x_1,0) &= \phi_2(x_1,1) = 0 & (8) \end{aligned}$$

and the Neumann boundary conditions

$$\left.\frac{\partial\phi_1}{\partial x_2}\right|_{(x_1,0)} = \left.\frac{\partial\phi_1}{\partial x_2}\right|_{(x_1,1)} = \left.\frac{\partial\phi_2}{\partial x_1}\right|_{(0,x_2)} = \left.\frac{\partial\phi_2}{\partial x_1}\right|_{(1,x_2)} = 0 \tag{9}$$

on the domain $\Omega = [0;1] \times [0;1]$, *Christensen* found the eigenfunctions to be

$$\begin{aligned} \boldsymbol{\phi}_{ij1} &= \alpha_1 \begin{bmatrix} i \sin i\pi x_1 \cos j\pi x_2 \\ j \cos i\pi x_1 \sin j\pi x_2 \end{bmatrix} & (10)\\ \boldsymbol{\phi}_{ij2} &= \alpha_2 \begin{bmatrix} -j \sin i\pi x_1 \cos j\pi x_2 \\ j \cos i\pi x_1 \sin j\pi x_2 \end{bmatrix} & (11) \end{aligned}$$

where the α's are determined so as to give the eigenfunctions unit energy. The corresponding eigenvalues are

$$\begin{aligned} \kappa_{ij1} &= -\pi^2\,(2\alpha+\beta)\,(i^2+j^2) & (12)\\ \kappa_{ij2} &= -\pi^2\,\alpha\,(i^2+j^2) & (13) \end{aligned}$$

If we locally describe the velocity by the eigenbasis $\boldsymbol{v} = \sum_{ijr} a_{ijr}\boldsymbol{\phi}_{ijr}$ and impose the viscous PDE (1) we obtain

$$\begin{aligned} \mathcal{L}\sum_{ijr} a_{ijr}\boldsymbol{\phi}_{ijr} + \boldsymbol{b} &= \boldsymbol{0} & (14)\\ \sum_{ijr} a_{ijr}\kappa_{ijr}\boldsymbol{\phi}_{ijr} + \boldsymbol{b} &= \boldsymbol{0} & (15)\\ < \sum_{ijr} a_{ijr}\kappa_{ijr}\boldsymbol{\phi}_{ijr} + \boldsymbol{b}\ ,\ \boldsymbol{\phi}_{kls} > &= < \boldsymbol{0}\ ,\ \boldsymbol{\phi}_{kls} > & (16)\\ a_{kls}\kappa_{kls} < \boldsymbol{\phi}_{kls}\ ,\ \boldsymbol{\phi}_{kls} > + < \boldsymbol{b}\ ,\ \boldsymbol{\phi}_{kls} > &= 0 & (17)\\ a_{kls} &= -\kappa_{kls}\ < \boldsymbol{b}\ ,\ \boldsymbol{\phi}_{kls} >, & (18) \end{aligned}$$

where we have projected the force onto the eigenfunction ϕ_{kls} and employed the normalization of the eigenfunctions to isolate the coefficient a_{kls} directly. To approximate the linear filter we position a unit force in the middle of the domain Ω and discretize to obtain the desired size of the filter. The sum of eigenfunctions is truncated appropriately in terms of the discretization, see *Gramkow* [7]. A $N \times N$ filter, low-pass filtered at the Nyquist frequency, is then calculated as

$$\boldsymbol{v}(\boldsymbol{x}) = \frac{4}{\alpha(2\alpha+\beta)\pi^2(N-1)^2} \cdot \sum_{i,j=0}^{N-1} \frac{\sin i\frac{\pi}{2} \cos j\frac{\pi}{2}}{(i^2+j^2)^2\Gamma(i,j)} \begin{bmatrix} (\alpha i^2 + (2\alpha+\beta)j^2) \sin i\pi x_1\ \cos j\pi x_2 \\ -(\alpha+\beta)\ ij \cos i\pi x_1\ \sin j\pi x_2 \end{bmatrix} \tag{19}$$

where

$$\boldsymbol{x} = \frac{1}{N-1}\boldsymbol{X} + \begin{bmatrix} 1/2 \\ 1/2 \end{bmatrix}, \tag{20}$$

$$\Gamma(i,j) = \begin{cases} 1 & \text{if } i \neq 0 \text{ and } j \neq 0 \\ 2 & \text{if } i = 0 \text{ or } j = 0 \end{cases}, \tag{21}$$

and $\boldsymbol{X}$ is the integer filter index. It is obvious that our approximation limits the scope of the forces to the size of the filters, but in turn we have a high order approximation of the deformation around the attacking point of the force. The limited scope of the forces is overcome by use of multi-resolution, i.e. image pyramids. In this survey we will compare the performance of the above filter and two other filters. The first filter is an optimal separation in the least-squares sense of (19) and the other filter is the well known gaussian, that has been used in a similar framework by *Thirion* [9]. Below we show the three filters.

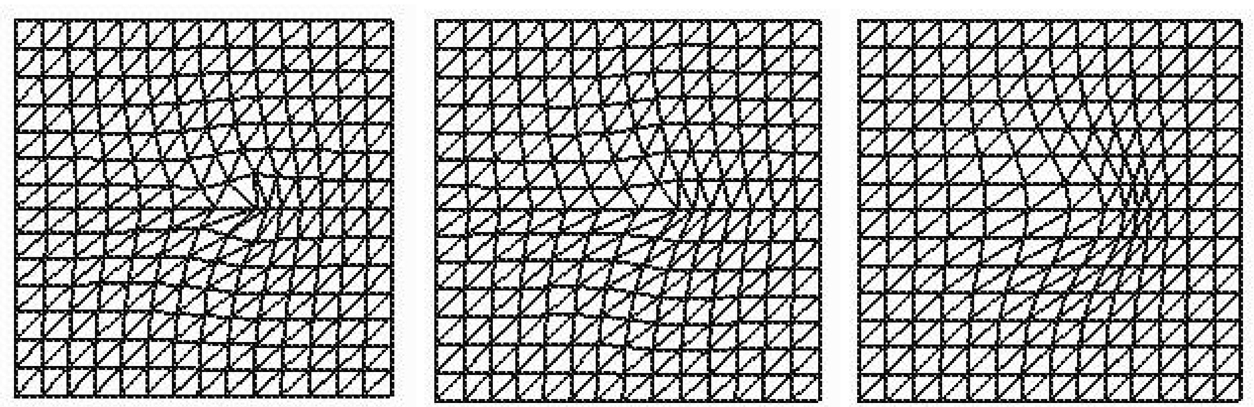

Figure 1: The figure shows the three compared filters. Left is the elastic filter (19), middle is the separated elastic filter, and right is the gaussian filter.

4 Results

The performance of three filters has been compared by registering two sets of images. Both registration problems are taken from *Christensen* [3]. All images are binary and of size 128×128. To avoid boundary problems the convolutions are performed on 256×256 padded images. The first problem is to register a Square to a Rectangle, and following we attempt to register a Circle to a C. The images are displayed below. The Square is 32×32 and the Rectangle is 32×64. The Circle has a radius of 31, and the C has an inner radius of 21, an outer radius of 41, and a gap that is 20 pixels wide.

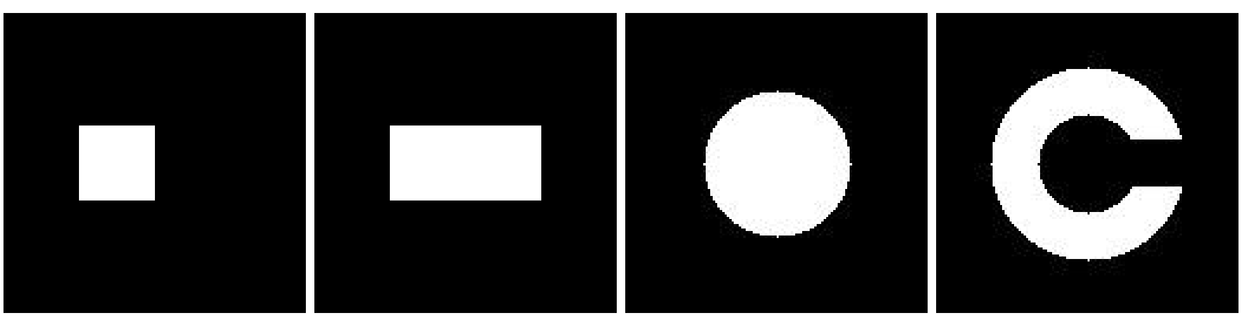

Figure 2: From left to right the images are: Square, Rectangle, Circle, and C.

The first registration problem is characterized by a large mass dilation and a large-distance parallel flow, whereas the Circle-to-C experiment serves to show the ability of the model to perform large-distance curved deformations. The results of the registration using the three different images are shown below. In order to track the individual particles the obtained deformation field has been imposed on a regular grid as well as on a textured version of the deforming image. The scope of the forces has been increased by performing the registration in multi-resolution.

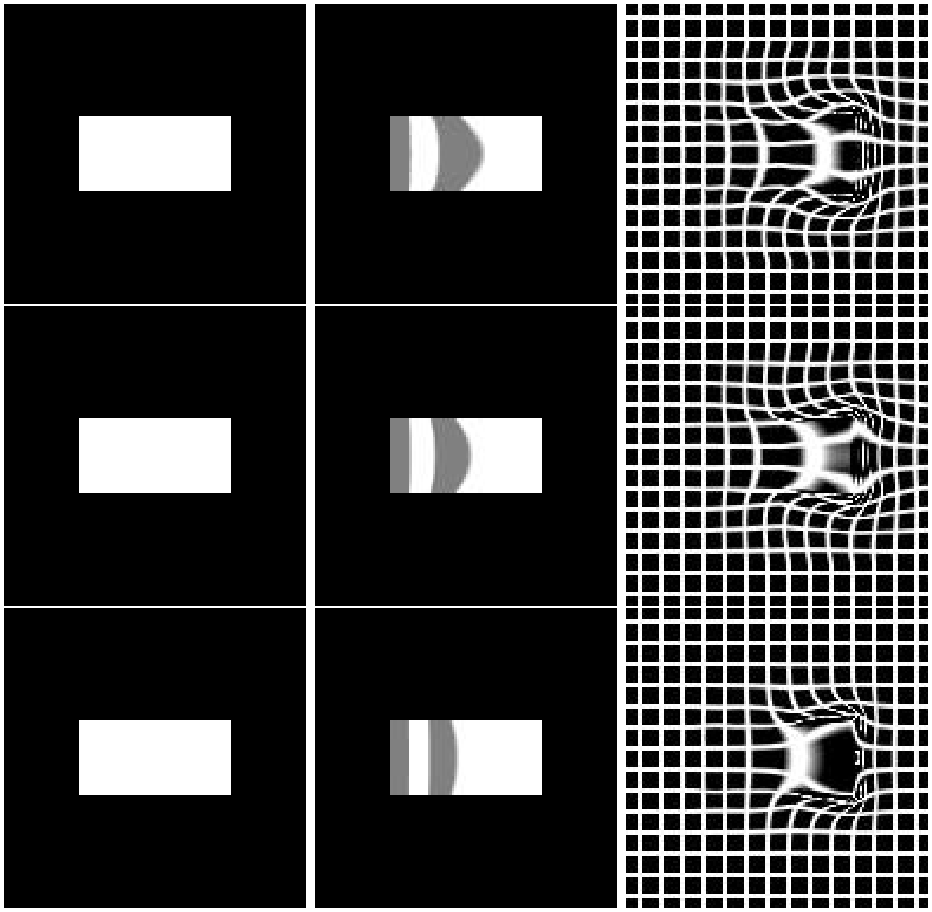

Figure 3: Square-to-Rectangle. The top to bottom rows show fluid registration using the elastic filter, the separated elastic filter, and the separated gaussian filter, respectively. The left column shows the deformed square, the middle column shows the deformation of a set of equally wide strips, and to the left the registration is displayed as applied to a grid.

It is obvious that the filter (19) yields the smoothest results. Note, how the resulting deformation influence a greater area in the upper images. As can be seen in the deformed grids this implies that the images, locally, are stretched less.

Note, in the Circle-to-C experiment, the well-mannered deformations of the concentric circles. The top row reveals that using the filter derived above these circles are deformed evenly, whereas the separated filter and the gaussian filter cause a decreased quality of the registration. The same tendency is seen on the deformed grids, which show that using the gaussian filter causes an excessive local dilation of the images.

In terms of a smooth flow there is no doubt that the derived filter is superior to the gaussian approximation. One might be surprised that the difference between the unseparated and the separated filter is so pronounced, considering the limited visual difference in figure 1. However, the explanation lies in the low signal-to-noise ratio of about 6 in the separation.

Both registration examples show that a complete registration can be obtained regardless of the used filter. This is perhaps a trivial observation, but it is important in the sense that the similarity between the deformed template and the study image does not ensure a reliable registration. This point justifies the use of Navier-Stokes equation (1), which favours deformations that are smooth and have a low change-rate of the divergence. These properties are relaxed in the separated filter, explaining the resulting lower quality of the registration when using this filter. The gaussian approximation is in many respects an unfortunate choice. Firstly, it has a flat tangent in origo, such that the point where the force is applied is shifted, with no contraction or dilation near the force. Instead, the maximal

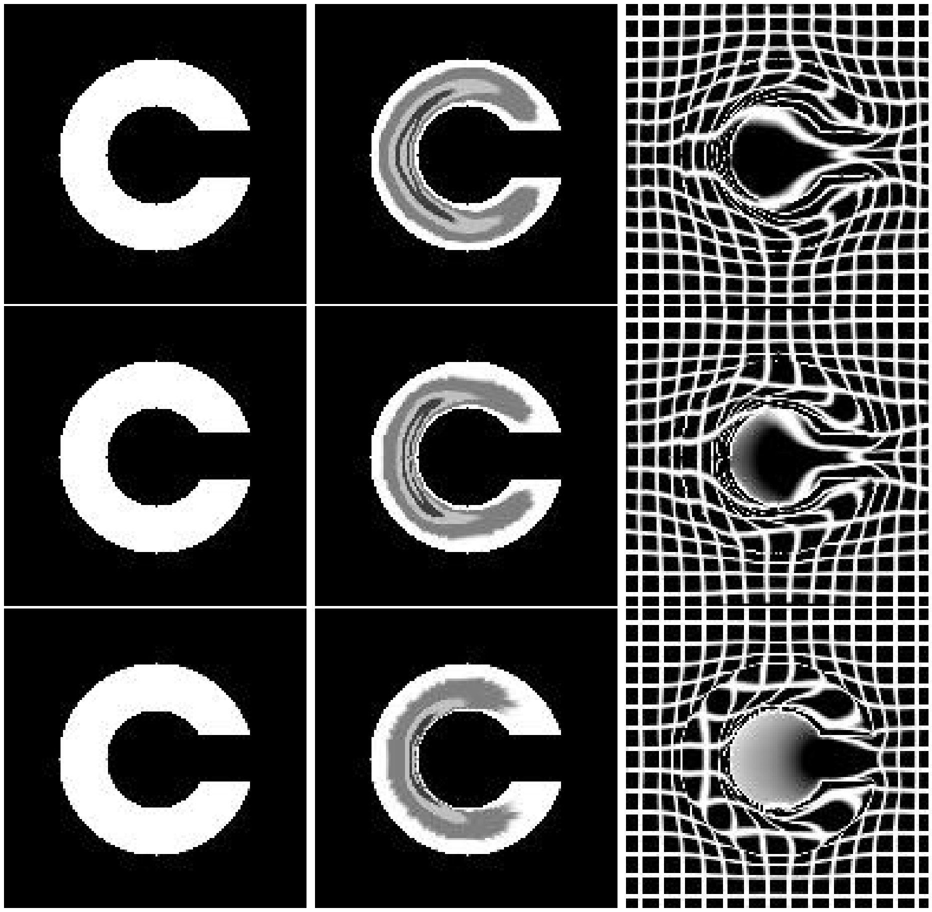

Figure 4: Circle-to-C. The top to bottom rows show fluid registration using the elastic filter, the separated elastic filter, and the separated gaussian filter, respectively. The left column shows the deformed circle, the middle column shows the deformation of a set of concentric circles, and to the left the registration is displayed as applied to a grid.

mass change occurs on the sides of the gaussian, where the derivatives have their maximum. Secondly, the gaussian yields no deformations orthogonal to the force. This cause a severe compression or expansion around the force, with limited propagation to the surrounding matter.

The Circle-to-C registration was performed in 180 secs. with our own filter (19) and 60 secs with the separated filters on a MIPS R5000 150MHz Silicon Graphics Indy. The Square-to-Rectangle registration runs slightly faster.

5 Conclusion

We have described a convolution solution to the Navier-Stokes equation, which is an important part of the fluid registration algorithm developed by *Christensen* [3]. Three different filters have been compared in terms of the smoothness of the deformation, that registers two images. It was shown that our filter performs satisfactorily, whereas a separated approximation and a simple gaussian filter, yield increasingly degenerated deformation fields. The main result in this paper is that the sensitivity in the registration to different regularization methods should not be underestimated. This is in particular seen between the registrations obtained by using the elastic filter and the gaussian filter, but the effect of separating the elastic filter is also visible. We note that the convolution approach is several times faster than the SOR algorithm in solving the viscous PDE and yields similar results on test images.

Acknowledgements

This work was performed while both authors were working at 3D-Lab, the Panum Institute. Professor Sven Kreiborg and staff are thanked for their support.

References

[1] Bajcsy, R. and Kovačič, *Multiresolution Elastic Matching*, Computer Vision, Graphics, and Image Processing 46, 1-21, 1989.

[2] Bro-Nielsen, M., Gramkow, C., *Fast Fluid Registration of Medical Images*, 3D-Lab, School of Dentistry, Univ. of Copenhagen, Nørre Allé 20, DK-2200 Copenhagen, Denmark, 1996.

[3] Christensen, G.E., *Deformable Shape Models for Anatomy*, Washington University, Sever Institute of Technology, Saint Louis, Missouri, August 1994.

[4] Christensen, G.E. et al., *Topological Properties of Smooth Anatomical Maps*, Proceedings of the 16th International Conference on Information Processing in Medical Imaging (IPMI'95), Ile de Berder, France, June 26-30, 1995.

[5] Christensen, G.E., Miller, M.I., and Vannier, M., *A 3D Deformable Magnetic Resonance Textbook based on Elasticity*, Department of Electrical Engineering, and The Institute for Biomedical Computing, Mallinckrodt Institute of Radiology, Washington University, Saint Louis, MO 63130, 1994.

[6] Christensen, G.E., Rabbitt, R.D., and Miller, M.I, *3D Brain Mapping using a Deformable Neuroanatomy*, The Institute for Biomedical Computing and The Electronic Signals and System Res. Laboratory, Washington University, Saint Louis, MO 63130, Phy. Med. Biol. 39, 1994, 608-618.

[7] Gramkow, C., *Registration of 2D and 3D Medical Images*, Master Thesis, Institute of Mathematical Modelling, DTU, DK. January 1996.

[8] Miller, M.I., Christensen, G.E., Amit, Y., and Grenander, U., *Mathematical Textbook of Deformable Neuroanatomics*, Proc. Natl. Acad. Sci. USA, Vol. 90, pp. 11944-11948, Medical Sciences, December 1993.

[9] Thirion, J.-P., *Fast Non-Rigid Matching of 3D Medical Images*, Institut International de Recherche en Informatique et en Automatique, France, April 1995.